Chemistry–A European Journal

Research Article
doi.org/10.1002/chem.202201649

Chemistry
Europe
European Chemical
Societies Publishing

www.chemeurj.org

Rational Tuning of the Reactivity of Three-Membered Heterocycle Ring Openings via S_N2 Reactions

Thomas Hansen,*[a, c] Alba Nin-Hill,[a] Jeroen D. C. Codée,[b] Trevor A. Hamlin,[c] and Carme Rovira*[a, d]

Abstract: The development of small-molecule covalent inhibitors and probes continuously pushes the rapidly evolving field of chemical biology forward. A key element in these molecular tool compounds is the "electrophilic trap" that allows a covalent linkage with the target enzyme. The reactivity of this entity needs to be well balanced to effectively trap the desired enzyme, while not being attacked by off-target nucleophiles. Here we investigate the intrinsic reactivity of substrates containing a class of widely used electrophilic traps, the three-membered heterocycles with a nitrogen (aziridine), phosphorus (phosphirane), oxygen (epoxide) or sulfur atom (thiirane) as heteroatom. Using quantum chemical approaches, we studied the conformational flexibility and nucleophilic ring opening of a series of model substrates, in which these electrophilic traps are mounted on a cyclohexene scaffold ($C_6H_{10}Y$ with Y = NH, PH, O, S). It was revealed that the activation energy of the ring opening does not necessarily follow the trend that is expected from C–Y leaving-group bond strength, but steeply decreases from Y = NH, to PH, to O, to S. We illustrate that the $HOMO_{Nu}$–$LUMO_{Substrate}$ interaction is an all-important factor for the observed reactivity. In addition, we show that the activation energy of aziridines and phosphiranes can be tuned far below that of the corresponding epoxides and thiiranes by the addition of proper electron-withdrawing ring substituents. Our results provide mechanistic insights to rationally tune the reactivity of this class of popular electrophilic traps and can guide the experimental design of covalent inhibitors and probes for enzymatic activity.

Introduction

Three-membered heterocycles (e.g., aziridines, phosphiranes, epoxides, thiiranes) are important building blocks in the toolbox of synthetic chemistry, finding broad application in many organic transformations. These three-membered heterocycles react with a wide range of nucleophiles in ring-opening reactions,[1] making them valuable building blocks for the synthesis of complex molecules used in a range of applications from polymer chemistry[2] to chemical biology.[3] In the last decades, they also have become an indispensable molecular tool for the detection, characterization, tracking and inhibition of cysteine proteases and carbohydrate processing enzymes.[3] Potent inhibitors are equipped with these "electrophilic traps", also known as "electrophilic warheads" or "reactive groups", which can covalently bind to a nucleophilic residue in the active site of the target enzyme (Figure 1a).

Understanding the intrinsic reactivity of electrophilic traps is essential for the rational design of potent and selective irreversible small molecule inhibitors. The electrophilic trap must balance between the appropriate reactivity and stability, trapping the target enzymes while leaving off-targets unscathed. Despite many active covalent inhibitors and probes that have been synthesized in the past, limited quantitative data are available regarding the impact of the nature and type of electrophilic traps on the ring-opening reaction.[5]

In general, aziridines have proven to be substantially more challenging to undergo ring-opening reactions than their corresponding epoxide counterpart in synthetic chemistry.[6] In sharp contrast, aziridine derivatives tend to react faster in enzymatic media, such as in the active sites of glycoside hydrolases, as the NH-group is primed for attack by protonation,[3] with some exceptions.[7] Significantly less is known about the reactivity of phosphiranes and thiiranes, while

[a] Dr. T. Hansen, Dr. A. Nin-Hill, Prof. Dr. C. Rovira
Departament de Química Inorgànica i Orgànica (Secció de Química Orgànica) &
Institut de Química Teòrica i Computacional (IQTCUB), Universitat de Barcelona
08028 Barcelona (Spain)
E-mail: t.hansen@ub.edu
c.rovira@ub.edu

[b] Prof. Dr. J. D. C. Codée
Leiden Institute of Chemistry, Leiden University
Einsteinweg 55, 2333 CC Leiden (The Netherlands)

[c] Dr. T. Hansen, Dr. T. A. Hamlin
Department of Theoretical Chemistry
Amsterdam Institute of Molecular and Life Sciences (AIMMS)
Amsterdam Center for Multiscale Modeling (ACMM)
Vrije Universiteit Amsterdam
De Boelelaan 1083, 1081 HV Amsterdam (The Netherlands)

[d] Prof. Dr. C. Rovira
Institució Catalana de Recerca i Estudis Avançats (ICREA)
08020 Barcelona (Spain)

Chem. Eur. J. 2022, 28, e202201649 (1 of 11)

© 2022 The Authors. Chemistry - A European Journal published by Wiley-VCH GmbH
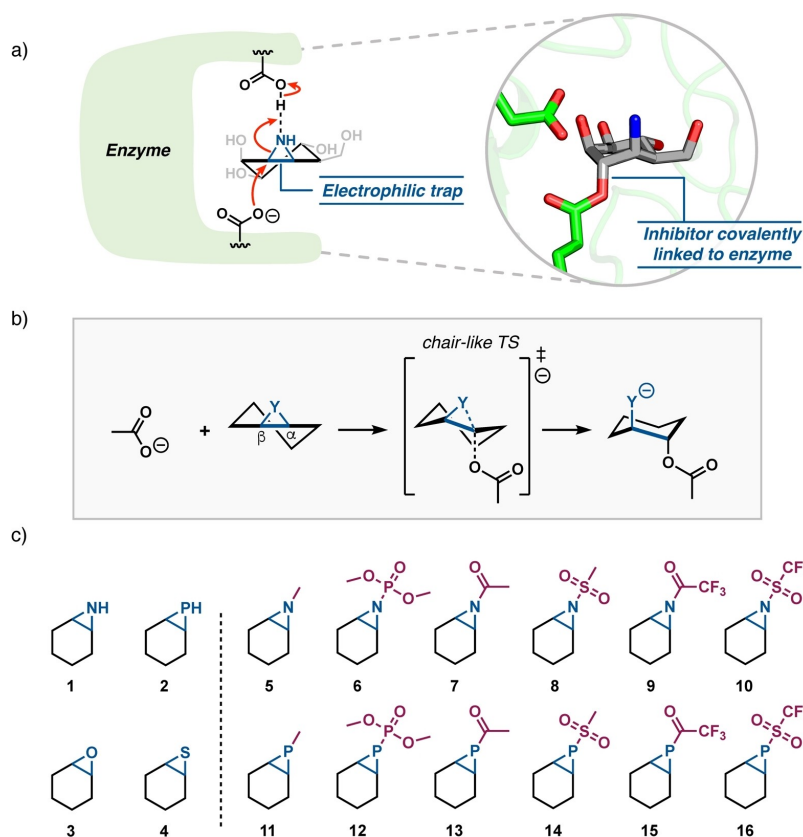
Figure 1. a) Generic operative mechanism of the ring-opening reaction of "electrophilic traps" in carbohydrate-active enzymes. The specific reaction shown corresponds to the labelling of a retaining glycosidase (PDB ID: 7OMS) by a mannose-configured epi-cyclophellitol-based aziridine. The exact mechanism naturally depends on many factors, for example, type and nature of the enzyme, the pH and the specific architecture of the inhibitor.[3c] b) Computationally analysed model ring-opening reactions by nucleophile AcO$^-$ with the lower-energy α-attack (chair-like transition state);[4] c) Library of studied substrates (**1**–**16**).

it has been suggested that thiiranes are more reactive than epoxides.[8] A deeper understanding of the chemistry of nucleophilic ring-opening reactions of these strained three-membered ring systems can guide the design of these irreversible enzyme inhibitors and probes.

In this work, we carried out a systematic investigation of the intrinsic reactivity of aziridines, phosphiranes, epoxides and thiiranes in ring-opening reactions by a nucleophilic carboxylate group, which is a typical nucleophile in an enzymatic glycosidase reaction and an archetypal nucleophile in synthetic chemistry. By studying the conformational flexibility and reaction energy profiles for ring-opening reactions of a series of model substrates **1**–**4**, we quantified the intrinsic effect of the type and nature of the substrate in these reactions. In model substrates **1**–**4**, the three-membered ring electrophile is mounted on a cyclohexene, that is, $C_6H_{10}Y$ with Y = NH, PH, O, S, (Figure 1b and c), as a model for the popular covalent cyclo-phellitol-type glycosidase inhibitors. We further investigated the effect of ring substituents[9] at the N and P atoms of the parent aziridine **1** and phosphirane **2** by using –Me, –P=O(OMe)$_2$, –COMe (acetyl; –Ac), –SO$_2$Me (mesyl; –Ms), –COCF$_3$ (trifluoroacetyl; –TFA), –SO$_2$CF$_3$ (triflyl; –Tf; Figure 1c; **5**–**16**).

Our results show that aziridines and phosphiranes display higher activation energies (lower reactivity) and hence react slower than epoxides and thiiranes, respectively. This reactivity trend can be traced back to the inherently higher energy of the LUMO of aziridines and phosphiranes, which engage in a weaker HOMO$_{Nu}$–LUMO$_{Substrate}$ interaction with the nucleophile, compared to epoxides and thiiranes. However, their reactivity can be tuned and being significantly enhanced by the addition of appropriate substituents on the aziridines and phosphiranes. Electron-withdrawing substituents are capable of effectively polarising the filled σ-orbitals of the substrate away from the incoming nucleophile, which results in a reduced steric (Pauli) repulsion between the substrate and nucleophile, and hence, lower activation energies, rendering these species more reactive than the corresponding epoxides and thiiranes.

Computational Methods

Conformational energy landscapes

For all computed conformational energy landscapes, quantum mechanical molecular dynamics (QM MD) simulations were

Chemistry–A European Journal

Research Article
doi.org/10.1002/chem.202201649

Chemistry Europe
European Chemical
Societies Publishing

performed with the CP2K 7.1 package,[10] which employs the QM program QUICKSTEP.[11] In line with previous works, the PBE functional[12] in the generalized gradient-corrected approximation of density functional theory (DFT) was used, which shows good performance in describing six-membered conformations.[13] A dual basis set of Gaussian and plane-waves (GPW) formalism was used.[11] The wave function was expanded in a Gaussian TZV2P basis set, which is of triple-ζ quality for all atoms and includes two polarization functions per element,[14] while an auxiliary plane-wave basis set with a cut-off of 300 Ry was used to converge the electron density. All QM MD simulations were performed in the NVT ensemble using an integration time step of 0.5 fs. The systems were firstly equilibrated without any constraint for at least 5 ps. Next, the metadynamics algorithm was activated to explore the conformation energy landscape of the substrate by the method provided by the Plumed 2.5.4 plugin.[15] Three collective variables (CVs) were included, qx/Q, qy/Q and qz/Q. The width of the Gaussian-shaped potential hills was set at 0.035, 0.030, 0.020 rad for qx/Q, qy/Q and qz/Q, respectively. The Gaussian height was set to 0.6 kcal mol^{-1}, while the time deposition interval between two consecutive Gaussians was set to 25 fs. For better convergence and accuracy, the Gaussian height was lowered to 0.1 kcal mol^{-1} upon the complete exploration of the FEL (after approx. 0.5 ns). The simulations were stopped after having added around 40 000 Gaussians (after ca. 1 ns; for specific values see Table S1 in the Supporting Information). Convergence was established according to the invariance of the energy differences between the principal wells of the reconstructed free energy surface along the simulation (standard deviation < 1 kcal mol^{-1}, considering the last 50 ps of simulation; Figures S4 and S5). The collective variables were reweighted to obtain the Cremer–Pople puckering coordinates[16] theta and phi (θ, φ) by the use of the Plumed driver 2.7.2.[15] Lastly, the data was visualized using a Mercator representation, which is an equidistant cylindrical projection that results in a rectangular map with respect to θ and φ. This diagram provides the conformational relationship among all conformations of a six-membered ring.[17]

Reaction profiles

For all computed reaction profiles, all calculations were performed using the Amsterdam Density Functional (ADF2019.305) software package.[18] The generalized gradient approximation (GGA) exchange-correlation functional OLYP was used for all computations, which consists of the optimized exchange (OPTX) functional proposed by Handy and co-workers,[19a] and the Lee−Yang−Parr (LYP) correlation functional.[19b] Our previous benchmark studies have shown that OLYP reproduces S_N2 barriers from highly correlated ab-initio studies to within only a few kcal mol^{-1}.[20] Scalar relativistic effects are accounted for using the zeroth-order regular approximation (ZORA).[21] The basis set used, denoted QZ4P, is of quadruple-ζ quality for all atoms and has been improved by four sets of polarization functions.[22] This large basis set is

required for small anionic species.[20] The accuracies of the fit scheme (Zlm fit) and the integration grid (Becke grid) were, for all calculations, set to VERYGOOD.[23] No symmetry constraints were used during the analyses. All calculated stationary points have been verified by performing a vibrational analysis calculation,[24] to be energy minima (no imaginary frequencies) or transition states (only one imaginary frequency). The character of the normal mode associated with the imaginary frequency of the transition state has been inspected to ensure that it is associated with the reaction of interest. The potential energy surfaces of the studied S_N2 reactions were obtained by performing intrinsic reaction coordinate (IRC) calculations,[25] which, in turn, were analysed using the PyFrag 2019 program.[26] The optimized structures were illustrated using CYLview.[27]

Activation strain and energy decomposition analysis

The activation strain model (ASM) of chemical reactivity,[28] also known as the distortion/interaction model,[29] is a fragment-based approach in which the potential energy surface (PES) can be described with respect to, and understood in terms of, the characteristics of the reactants, that is, the nucleophile and substrate. It considers the rigidity of the reactants and to which extent they need to deform during the reaction, plus their capability to interact with each other as the reaction proceeds. With the help of this model, we decompose the total energy at a given state (ζ) along the reaction coordinate, $\Delta E(\zeta)$, into the strain and interaction energy, $\Delta E_{strain}(\zeta)$ and $\Delta E_{int}(\zeta)$, respectively, and project these values onto the reaction coordinate ζ [Eq. (1)].

$$\Delta E(\zeta) = \Delta E_{strain}(\zeta) + \Delta E_{int}(\zeta) \tag{1}$$

In this equation, the strain energy, $\Delta E_{strain}(\zeta)$, is the penalty that needs to be paid in order to deform the reactants from their equilibrium to the geometry they adopt during the reaction at point ζ of the reaction coordinate. The interaction energy, $\Delta E_{int}(\zeta)$, accounts for all the chemical interactions that occur between these two deformed reactants along the reaction coordinate.

The interaction energy between the deformed reactants can be further analysed in terms of quantitative Kohn−Sham molecular orbital (KS-MO) theory together with a canonical energy decomposition analysis (EDA).[30] The EDA decomposes the $\Delta E_{int}(\zeta)$ into the following three energy terms [Eq. (2)]:

$$\Delta E_{int}(\zeta) = \Delta V_{elstat}(\zeta) + \Delta E_{Pauli}(\zeta) + \Delta E_{oi}(\zeta) \tag{2}$$

Here, $\Delta V_{elstat}(\zeta)$ is the classical electrostatic interaction between the unperturbed charge distributions of the (deformed) reactants and is usually attractive. The Pauli repulsion, $\Delta E_{Pauli}(\zeta)$, includes the destabilizing interaction between the occupied orbitals of both fragments due to the Pauli principle. The orbital interaction energy, $\Delta E_{oi}(\zeta)$, accounts for, amongst others, charge transfer between the fragments, such as HOMO–LUMO interactions.

Chemistry–A European Journal

Research Article
doi.org/10.1002/chem.202201649

Chemistry Europe
European Chemical
Societies Publishing

In the activation strain and accompanied energy decomposition diagrams presented here, the energy terms are projected onto the carbon-leaving group ($C^\alpha \cdots Y$) bond stretch. This critical reaction coordinate undergoes a well-defined change during the reaction from the reactant complex via the transition state to the product and has been shown to be a valid reaction coordinate for studying S_N2 reactions.[4,31]

Results and Discussion

Structure and reactivity trends

The conformational flexibility of the $C_6H_{10}Y$ (Y = NH, PH, O, S) substrates is limited due to their 6- and 3-membered fused rings, which flattens the six-membered ring structures. Identifying the most stable conformation and the possible existence of competing conformations is important to accurately model the reactivity of the overall ring-opening reaction. To this end, we computed the conformational free energy landscape (FEL) of substrates 1–4 with respect to Cremer–Pople ring puckering coordinates (θ and φ) by ab-initio metadynamics (see Computational Methods for more details).

The FEL of aziridine 1 and epoxide 3 is shown in Figure 2, and those of phosphirane 2 and thiirane 4 are shown in Figure S1. The flattened $^3H_4$ and $^4H_3$ half chair conformations are most favoured, which for these substrates are chemically equivalent. This is in agreement with the neutron powder diffraction data of epoxide 3.[32] These conformations are also in line with experimental structures found for unreacted electrophilic traps in the active site of enzymes.[7,33] These local minima can relatively easily interconvert via a boat conformation ($^{2,5}B$ and $B_{2,5}$). In all cases, interconversion via the $B_{2,5}$ follows a lower energy pathway than interconversion via $^{2,5}B$, as the former bends both flagpole hydrogens away from the fused three-membered ring (see also Table S2). For example, aziridine 1 has an energy of 3.7 and 5.1 kcal mol^{-1} for $B_{2,5}$ and $^{2,5}B$, respectively. This behaviour is also found for more decorated 6- and 3-membered fused ring systems.[33c]

Conformational energy barriers do not vary much for the different types of three-membered heterocycles (3.7, 3.4, 3.6, 1.2 kcal mol^{-1} for Y = NH (1), PH (2), O (3), S (4), respectively). Noteworthy, these results are in excellent agreement with the previously obtained interconversion barrier of 4.2 kcal mol^{-1} estimated from NMR experiments for epoxide 3.[34] Introducing ring substituents at the N or P atom of aziridine 1 and phosphirane 2, respectively, does not change the qualitative shape of the FEL of the parent substrates, in which the $^3H_4$- and $^4H_3$-like conformations are most favoured (Figures S2 and S3). Altogether, the conformational energy landscapes show that all substrates are expected to react from $^3H_4$- or $^4H_3$-like conformations, which we have used to compute reaction profiles of their corresponding ring-opening reactions.

The computed reaction profiles for the ring-opening reactions of substrates 1–16 are collected in Table 1 and Figure 3 at ZORA-OLYP/QZ4P (reactivity trends are consistent for ΔE and ΔG; Table S3). Note that we also computed all

Table 1. Energies relative to the separate reactants [kcal mol^{-1}] of the stationary points (RC = reactant complex, TS = transition state and P = reaction product) of ring-opening reactions of 1–16 + AcO$^-$.[a]

Substrate	RC (ΔE_{RC})	TS ($\Delta E^{\ddagger}$)	P (ΔE_P)
1 (Y = NH)	−5.5	32.1	29.6
2 (Y = PH)	−7.3	21.2	17.2
3 (Y = O)	−7.6	16.6	8.8
4 (Y = S)	−8.9	9.6	1.4
5 (Y = NMe)	−6.5	31.8	28.0
6 (Y = NP=O(OMe)$_2$)	−10.5	11.0	−8.2
7 (Y = NAc)	−12.2	10.1	−9.7
8 (Y = NMs)	−13.7	7.0	−13.7
9 (Y = NTFA)	−13.9	0.5	−24.8
10 (Y = NTf)	−14.3	−2.7	−29.3
11 (Y = PMe)	−8.4	25.9	23.1
12 (Y = PP=O(OMe)$_2$)	−10.8	8.5	−4.8
13 (Y = PAc)	−10.4	6.0	−6.6
14 (Y = PMs)	−15.0	6.9	−5.9
15 (Y = PTFA)	−11.7	−3.3	−20.0
16 (Y = PTf)	−13.9	−0.7	−18.0

[a] Electronic energies computed at the ZORA-OLYP/QZ4P level of theory.

systems at ZORA-PBE/TZ2P (employed in the FEL computations), which gives exactly the same reactivity trends (Table S4). All reactions proceed from the separate reactants forming a reactant complex (RC), which evolves towards the product (P) through a chair-like transition state (TS). The precise conformational itinerary that the substrate follows along the ring-opening reaction, plotted onto the conformational FEL (Figure 2a and c), shows that the substrate gradually evolves from a half chair to a chair. Of note, we also computed the skew-boat-like transition state (β-attack) of all substrates (Table S5) and found, in line with our previous work,[4] that this pathway is substantially higher in energy and thus not relevant.

Several clear reactivity trends emerged from the computed reaction energy barriers (Table 1). First, the activation energy steeply decreases across the series Y = NH (1), PH (2), O (3), S (4) in $C_6H_{10}Y$ ($\Delta E^{\ddagger}$ = 32.1, 21.2, 16.6, 9.6 kcal mol^{-1}, respectively). This corroborates the notion that aziridines are intrinsically more challenging to undergo ring-opening reactions than the corresponding epoxides ($\Delta\Delta E^{\ddagger}$ = +15.5 kcal mol^{-1} for aziridine 1 with respect to epoxide 3).[6] Accordingly, the products of the ring-opening become more stabilized across this same series (ΔE_P = 29.6, 17.2, 8.8, 1.4 kcal mol^{-1}, respectively). Therefore, both from a kinetic and thermodynamic point of view, the efficiency of the ring-opening increases going from Y = NH, to PH, to O, to S. Hence, both by going down a group in the periodic table for the Y atom in the C^α–Y leaving-group bond of the substrate (Y = NH to PH or Y = O to S) or across a period (Y = NH to O or Y = PH to S) the ring-opening activation energy significantly decreases.

Our results also show that the introduction of ring substituents (−Me, −P=O(OMe)$_2$, −Ac, −Ms, −TFA, −Tf; 5–16) at the N or P atom of aziridine 1 and phosphirane 2 can significantly lower the activation energy of the corresponding nucleophilic ring-opening reaction. For example, the activation energy significantly decreases from Y = NH (1), to NMs, (8) to NTf (10) in $C_6H_{10}Y$ (with $\Delta E^{\ddagger}$ = 32.1, to 7.0, to −2.7 kcal mol^{-1}; $\Delta\Delta E^{\ddagger}$ = −34.8 kcal mol^{-1} for aziridine 10 with respect to the
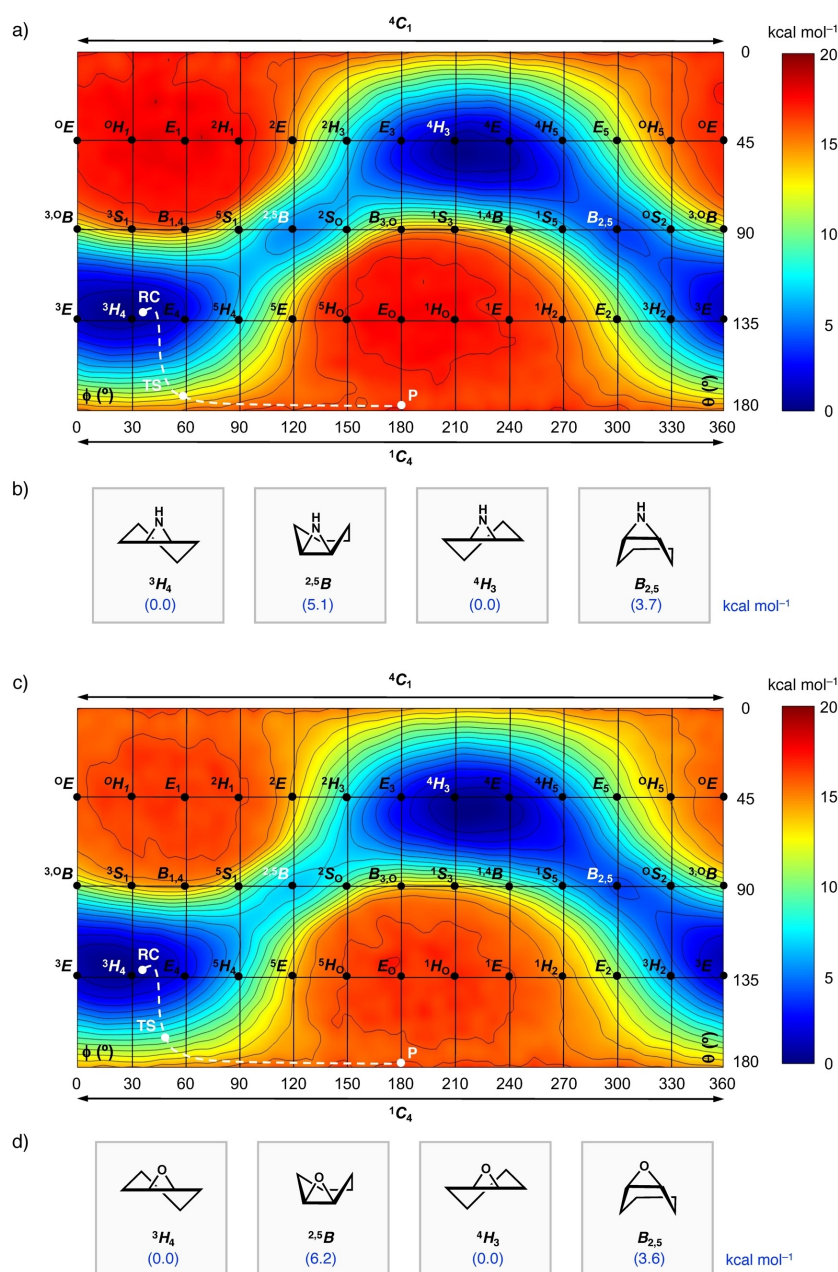
Chem. Eur. J. 2022, 28, e202201649 (4 of 11)

© 2022 The Authors. Chemistry - A European Journal published by Wiley-VCH GmbH

Chemistry–A European Journal

Research Article
doi.org/10.1002/chem.202201649

Chemistry Europe
European Chemical
Societies Publishing

Figure 2. Conformational FEL of a) aziridine **1** and c) epoxide **3**, which adopt $^3H_4$ and $^4H_3$ conformations with the corresponding conformational itinerary along the ring-opening reaction (RC = reactant complex, TS = transition state, and P = reaction product). The x- and y-axes correspond to the φ and θ Cremer–Pople puckering coordinates [°], respectively. Isolines are 1 kcal mol^{-1}. Relevant low-energy structures with their respective free energy of b) **1** and d) **3**.

parent aziridine **1**). Note that the overall activation energy $\Delta E^{\pm}$, that is, the energy difference between the TS and the separated reactants can be negative, as in the case of **10**, **15** and **16**, if a substantially stabilized reactant complex is formed. This typically occurs in apolar, weakly solvating solvents and, especially, in the gas phase (see ref. 35 for a more detailed discussion). Importantly, only electron-withdrawing groups, that is, −P=O(OMe)$_2$, −Ac, −Ms, −TFA and −Tf, are capable of substantially lowering the activation energy, while an alkyl-group, Y = NMe (**5**), leads to a similar barrier as found for the parent aziridine **1** (Y = NH). In the case of aziridines, the barrier

reduction correlates well with the electron-withdrawing capability of the substitutions going from −Ac, to −Ms, to −TFA, to −Tf.[36] The products of the ring-opening reaction also become more stabilized across this series.

To understand the role of solvation on the reactivity trends, we computed all reaction profiles in bulk solution with the use of COSMO (Tables S6 and S7).[37] We selected dichloromethane ($\varepsilon = 9$, nonpolar aprotic) and water ($\varepsilon = 78$, polar protic), spanning realistic extremes of polarity found in experimental work. Generally, a polarity of $\varepsilon \approx 4$,[38,39] is considered for enzymatic environments, which is in between the polarity of

Chemistry–A European Journal

Research Article
doi.org/10.1002/chem.202201649

Chemistry Europe
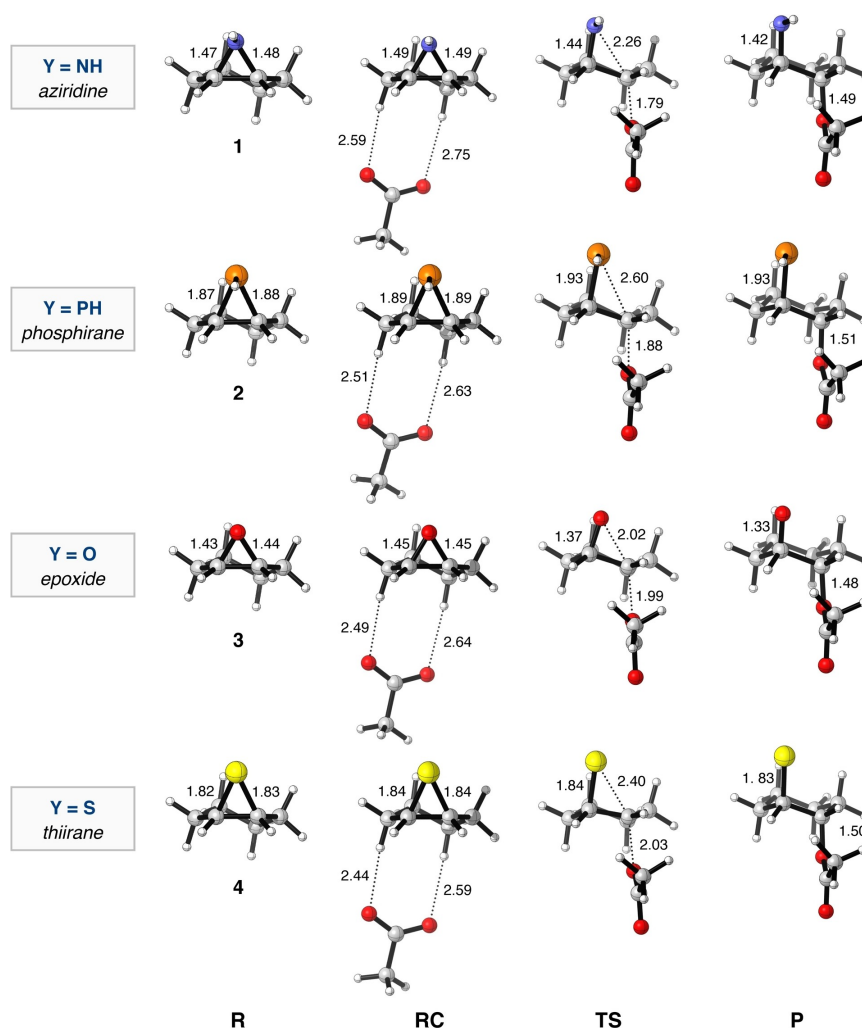European Chemical
Societies Publishing

Figure 3. Structures and key distances [Å] of stationary points (R = reactant, RC = reactant complex, TS = transition state and P = reaction product) of the ring-opening reactions of **1–4** + AcO⁻, computed with ZORA-OLYP/QZ4P. Atom colors: carbon (gray), hydrogen (white), nitrogen (blue), oxygen (red), phosphorus (orange) and sulfur (yellow).

the gas phase and dichloromethane. In line with our previous work,[31f] we find that bulk solvation increases all activation energies due to the stabilization of the anionic nucleophile, AcO⁻, and hence, decreasing its electron-donating capabilities. This effect becomes more apparent by going to more polar solvents. For example, the activation energy of the ring-opening reaction of epoxide **3** increases $\Delta E^{\pm} = 16.6$, to 30.4, to 31.5 kcal mol⁻¹ going from the gas phase, to dichloromethane, to water. Importantly, solvation renders identical intrinsic reactivity trends as found in the gas phase for the set of electrophilic traps.

Activation strain analyses

To gain quantitative insight into the effect of the type and nature of the leaving group in the nucleophilic ring-opening reactions, we analysed the energy changes along the reaction coordinate using the activation strain model. As detailed in the

Computational Methods, this fragment-based approach decomposes the total electronic energy (ΔE), as found in Table 1, into two chemically intuitive and useful terms: i) the developing destabilizing strain (distortion; ΔE_{strain}) and ii) stabilizing interaction energy (ΔE_{int}) along the reaction, which proved to be a valuable tool for understanding activation energies, and hence chemical reactivity.[31,40] Figure 4 shows the activation strain diagrams for substrates **1–4** in four panels: a) Y = NH vs. PH, b) Y = O vs. S, c) Y = NH vs. O and d) Y = PH vs. S. In both Figure 4a and 4b, the leaving-group atom varies going down a group in the periodic table (from NH to PH, or O to S). As we already discussed, the activation barrier (indicated by a solid circle) significantly decreases going from Y = NH to PH and O to S. This stems from the less destabilizing strain, which is illustrated by the orange and yellow strain energy curves, that are below their blue and red counterparts. In line with our recent work on S_N2 reactivity,[31b] the observed diminished destabilizing strain by going down in the group of the periodic table for the Y atom in the C^α−Y bond can be directly traced back to the weaker bond
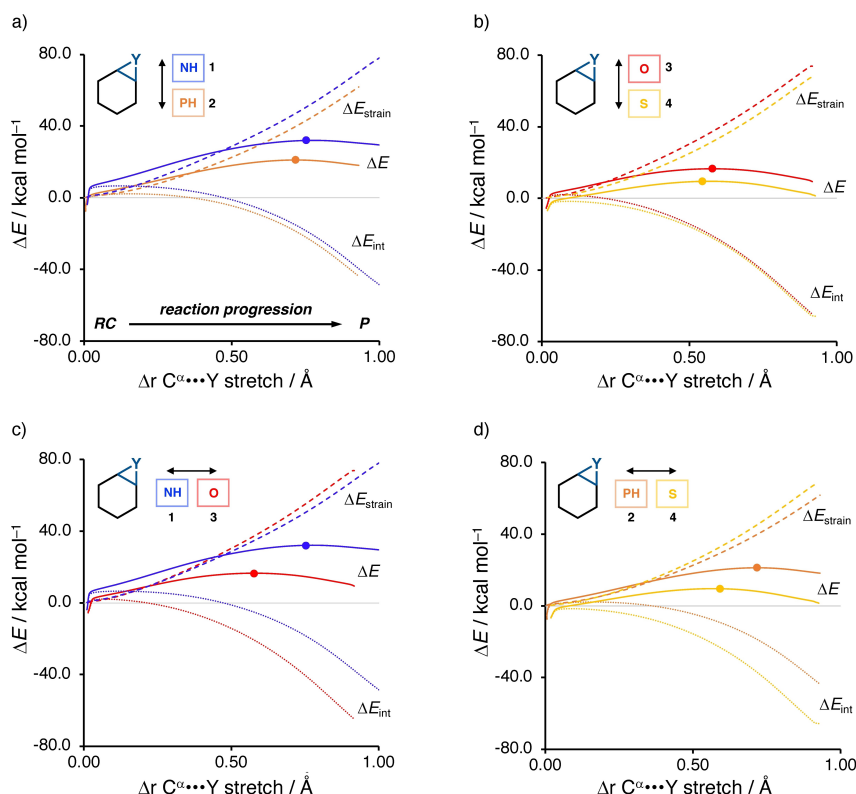
Chemistry–A European Journal | Research Article
doi.org/10.1002/chem.202201649

Chemistry
Europe
European Chemical
Societies Publishing

Figure 4. Activation strain analysis for the ring-opening of **1–4** + AcO⁻, along the IRC projected onto the Cᵅ···Y bond stretch (RC = reactant complex and P = reaction product). Transition states are indicated as filled circles on the curves. Trends across the first row (a and b) show the influence on the reactivity going down a group for the Y atom in the Cᵅ–Y bond, whereas trends across the second row (c and d) show how variation across the period influences the reactivity. Computed at the ZORA-OLYP/QZ4P level of theory.

strength (Figure 6a). For example, in line with experimental data,[41] the C–N bond strength for aziridine **1** is $\Delta H_{BDE} = 53.7 \text{ kcal mol}^{-1}$, whereas the bond strength is significantly weaker for the C–P bond: $\Delta H_{BDE} = 43.3 \text{ kcal mol}^{-1}$ for phosphirane **2** (see Table S8 for computed ΔH_{BDE} of all systems). Consistently, the bond becomes significantly longer, going from aziridine **1** (Cᵅ–N = 1.48 Å) to phosphirane **2** (Cᵅ–P = 1.88 Å). Recently, an explanation for the underlying physical mechanism behind the weakening of the C–Y bond going down a group for the Y atom has been provided. The C–Y bond becomes weaker and longer due to the increase in atom size by going down a group, which introduces more steric repulsion between the C and Y groups.[42]

When we vary the leaving-group across a period, that is, shifting horizontally in the periodic table (from N to O and from P to S; Figure 4c and d), the activation energy also decreases, however, in this case, this is due to the significant increase in stabilizing interaction energy between the nucleophile and substrates. Figure 4c and d shows that the interaction energy curves for epoxide **3** and thiirane **4** (red for **3** and yellow for **4**), are below the corresponding values for aziridine **1** and phosphirane **2** (blue for **1** and orange for **2**), respectively. In contrast, the strain curves exhibit an opposite trend with respect to the total energy (the strain becomes more destabilizing across the period),[43] and these thus do not explain the observed reactivity differences.

The reason why epoxide **3** and thiirane **4** benefit from a substantially more stabilizing interaction, compared to aziridine **1** and phosphirane **2**, is due to the significantly lower-lying LUMO (i.e., more stabilized LUMO), which has mainly σ* antibonding character in the Cᵅ–Y leaving-group bond, (Figures 5a and S6). This is a direct effect of the steep decrease in energy of the atomic orbitals (AOs) of the Y atom moving across a period, pulling down the σ* C–Y LUMO. Note that the C–Y bond also shortens and strengthens across a period.[42] Ultimately, the lower energy LUMO gives epoxide **3** a better electron-accepting capability than aziridine **1**, which engages in a more stabilizing HOMO–LUMO interaction with the incoming nucleophile (Figure 6b). This results in a more stable TS and, thus, a lower activation energy (see Figure S7 for all EDA plots and Table S9 for ASM/EDA data on consistent geometries).

The more stabilizing interaction energy, when varying the leaving-group across a period, is reinforced by the stronger electrostatic interactions between the reactants (Figure 5b). The more electron-withdrawing character of the O atom of epoxide **3** compared to the N atom of aziridine **1** results in more δ⁺ on the electrophilic Cᵅ atom (see Figure S8 for data), which leads to a strengthening of the electrostatic interaction with the incoming negatively charged nucleophile AcO⁻.

After having established the origin of the reactivity differences between the different type of three-membered heterocycles, we analysed the effect of the introduction of electron-
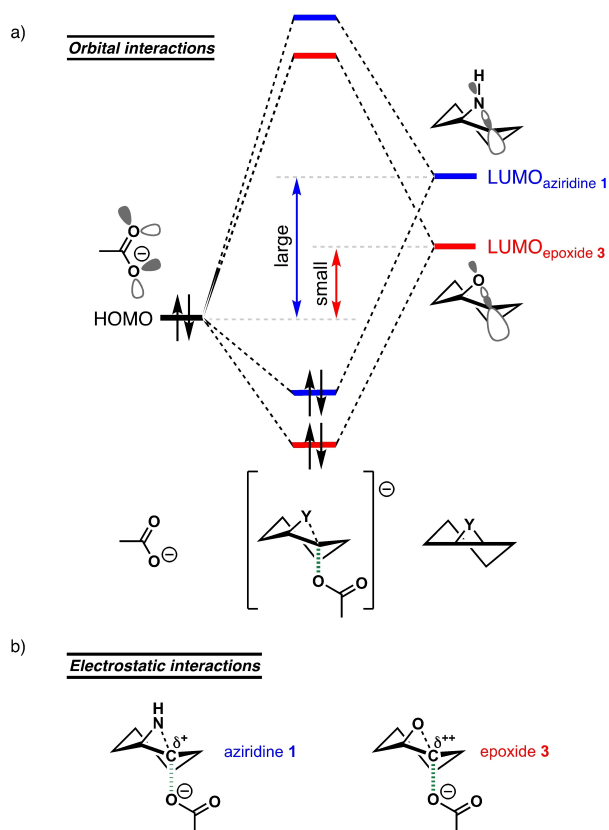
Chemistry–A European Journal

Research Article
doi.org/10.1002/chem.202201649

Chemistry Europe
European Chemical
Societies Publishing

Figure 5. a) Schematic molecular orbital diagram of the key HOMO$_{Nu}$–LUMO$_{Substrate}$ orbital interaction and b) schematic molecular electrostatic potential map for the ring opening of aziridine **1** and epoxide **3** + AcO⁻.
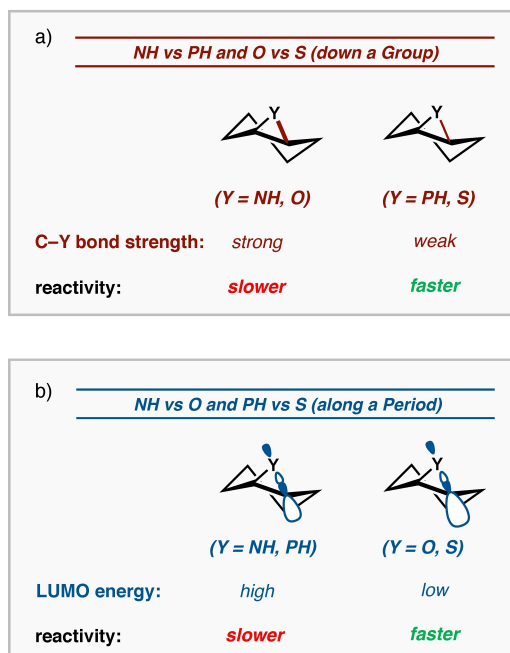

Figure 6. Schematic summary of the main factors governing the intrinsic reactivity of the substrate for a) NH vs. PH and O vs. S (going down a group in the periodic table); b) NH vs. O and PH vs. S (across a period).

withdrawing ring substituents, that is, −P=O(OMe)₂, −Ac, −Ms, −TFA and −Tf, at the N and P atoms of parent aziridine **1** and phosphirane **2**. In this section, we focus on the ring-opening of parent aziridine **1** (Y=NH) and substituted aziridine **8** (Y=NMs) and **10** (Y=NTf) by AcO⁻. Importantly, all the other systems featuring electron-withdrawing groups share similar characteristics and can be found in Figures S9 and S10. As shown in Figure 7a, the lower activation energy for the substituted aziridine **8** and **10** is the result of a more stabilizing interaction energy between the nucleophile and substrate, while the strain energy is very similar for all systems. The strain energy curves can be traced back to the almost equal bond strength of the corresponding C$^\alpha$−Y bonds (ΔH_{BDE}= 53.7, 52.5 and 53.1 kcal mol⁻¹ for aziridine **1**, **8** and **10**, respectively). One could expect a less destabilizing strain for the substituted aziridines **8** and **10**, since these groups can effectively stabilize the build-up of negative charge of the leaving group atom, therefore making it easier to break the C$^\alpha$−Y bond. However, we found that this effect is counterbalanced by the fact that these relatively large groups adopt an axial orientation in the ring-opened products, which introduces destabilizing steric repulsion with the ring protons.

The energy decomposition analysis (EDA) for substrates **1**, **8** and **10** across the reaction (Figure 7b; see Computational Methods for more details) shows that the more stabilizing interaction energy between the substrate and nucleophile for the substituted aziridines **8** and **10** can be traced back to a less destabilizing steric (Pauli) repulsion between the nucleophile and substrate along the complete reaction coordinate. The diminished destabilizing steric (Pauli) repulsion for substituted aziridine **8** and **10** compared to **1** originates from the polarization of the filled σ-orbitals of the substrate by the electron-withdrawing groups away from the incoming nucleophile (Figure 7c). In particular, the FMO$_{substrate}$ presenting a filled σ-bonding orbital predominantly located on the C$^\alpha$−N bond, of the aziridine (HOMO for **1** and **8** and HOMO−2 for **10**), is in the way of incoming nucleophile (see Figure S11 for data), and the electron-withdrawing groups can move a portion of the orbital amplitude away from the incoming nucleophile. Intuitively, the magnitude of this effect is dictated by the strength of the electron-withdrawing group, which increases going from NMs (**8**) to NTf (**10**).

This operative mechanism is closely related to our recently introduced Pauli repulsion-lowering catalysis,[4,44] which is operational in several Lewis acid-catalysed transformations, spanning from nucleophilic substitutions and additions to cycloaddition reactions. In Lewis acid-catalysed reactions, non-covalent interactions play a major role in causing the reduction of steric (Pauli) repulsion between the reactants. Here we have shown for the first time that it is also possible to have the exact operative mechanism through a covalently linked group to the substrate rather than an exogenous catalyst.

The interaction energy trend is reinforced by the attractive orbital interaction, which is more stabilizing for the substituted aziridine **8** and **10**, which can be traced back to the more stabilized LUMO of the substrate, leading to a smaller HOMO–LUMO gap with the incoming nucleophile (see Table S10 for
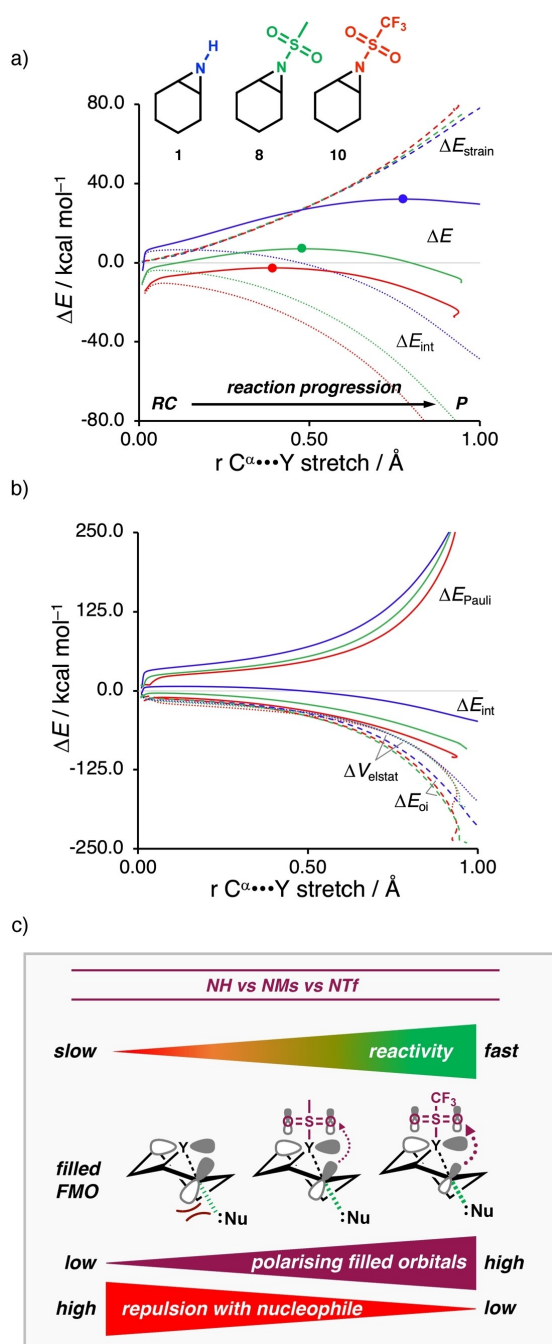
Figure 7. a) Activation strain analysis and b) energy decomposition analysis for the ring opening of **1** (blue), **8** (green) and **10** (red) + AcO⁻, along the IRC projected onto the $C^\alpha \cdots Y$ bond stretch. Transition states are indicated with dots. c) Schematic summary of the main factors determining the reactivity of the substrate when electron-withdrawing ring substituents are introduced at the N or P atom of parent aziridine **1** and phosphirane **2**.

ASM/EDA data on consistent geometries). This effect stems from the electron-withdrawing character of the substituent, which lowers the substrate's LUMO. Likewise, as for the Pauli repulsion reduction, the magnitude of this effect is dictated by the strength of the electron-withdrawing group.

Conclusion

Our computational investigation reveals that the activation energy for the ring opening of three-membered heterocycles mounted on a cyclohexene scaffold, that is, $C_6H_{10}Y$, significantly decreases on going down a group in the periodic table for the Y atom in the C–Y leaving-group bond (Y = NH to PH, or O to S) or across a period (Y = NH to O, or PH to S). In addition, we have shown that it is possible to tune the activation energy of the less-reactive aziridines and phosphines far below that of the corresponding epoxide and thiiranes by introducing electron-withdrawing ring substituents, for example, –COMe (–Ac), –SO₂Me (–Ms), –SO₂CF₃ (–Tf), directly at the nitrogen or phosphorus.

Our activation strain and energy decomposition analyses helped to rationalize these results, showing that the lower activation energy upon going down a group (Y = NH to PH, or O to S) stems from a less destabilizing strain energy, which is a direct result of the substantially weaker C–P and C–S leaving-group bond. The C–Y bond significantly weakens going down a group due to the increased atom size, introducing more repulsion between the C and Y groups. In contrast, the lower activation energy upon moving across a period (Y = NH to O, or PH to S) stems from an enhanced orbital interaction between the nucleophile and substrate, namely, the LUMO of the substrates with C–O and C–S leaving-group bonds is lower in energy, engaging in a stronger HOMO_Nu–LUMO_Substrate.

We found that the lower activation barrier of aziridines and phosphiranes with electron-withdrawing groups at the nitrogen or phosphorus is caused by a diminished destabilizing steric (Pauli) repulsion between the substrate and nucleophile, and not by weakening of the C–Y leaving-group bond. The electron-withdrawing substituents are capable of effectively polarising the filled orbitals of the aziridine away from the incoming nucleophile. The nucleophile–substrate interaction is further reinforced by the low-lying LUMO of these substrates resulting in a more favourable orbital interaction with the nucleophile. Our results could be useful in synthetic chemistry for more effectively employing these strained three-membered ring systems, which are essential building blocks for many chemical transformations. At the same time, the mechanistic insights provided in our work will help to rationally tune the reactivity of three-membered ring electrophilic traps and, in doing so, guide the design of irreversible inhibitors and probes for enzymatic activity.

Supporting Information

Additional computational results; Cartesian coordinates, energies and the number of imaginary frequencies of all stationary points.

Chemistry–A European Journal | Research Article
doi.org/10.1002/chem.202201649

Chemistry
Europe
European Chemical
Societies Publishing

Acknowledgements

Conflict of Interest

The authors declare no conflict of interest.

Data Availability Statement

The data that support the findings of this study are available in the supplementary material of this article.

[1] a) A. Padwa, S. Murphree, *Arkivoc* **2006**, *3*, 6; b) J. G. Smith, *Synthesis* **1984**, *1984*, 629; c) P. Crotti, M. Pineschi in *Aziridines and Epoxides in Organic Synthesis*, Wiley, Hoboken, **2006**, pp. 271–313; d) S. R. Pathipati, V. Singh, L. Eriksson, N. Selander, *Org. Lett.* **2015**, *17*, 4506–4509.

[2] a) C. Schneider, *Synthesis* **2006**, *23*, 3919; b) I. Vilotijevic, T. F. Jamison, *Angew. Chem.* **2009**, *121*, 5362; *Angew. Chem. Int. Ed.* **2009**, *48*, 5250; c) A. Rolfe, T. B. Samarakoon, P. R. Hanson, *Org. Lett.* **2010**, *12*, 1216; d) B. M. Loertscher, Y. Zhang, S. L. Castle, *Beilstein J. Org. Chem.* **2013**, *9*, 1179; e) H. Kudo, S. Makino, A. Kameyama, T. Nishikubo, *Macromolecules* **2005**, *38*, 5964–5969; f) A. Takahashi, R. Yuzaki, Y. Ishida, A. Kameyama, *J. Polym. Sci. A: Polym. Chem.* **2019**, *57*, 2442–2449; g) N. Spassky, A. Momtaz, A. Kassamaly, M. Sepulchre, *Chirality* **1992**, *4*, 295–299; h) E. Rieger, A. Manhart, F. R. Wurm, *ACS Macro Lett.* **2016**, *5*, 195–198; i) I. C. Stewart, C. C. Lee, R. G. Bergman, F. D. Toste, *J. Am. Chem. Soc.* **2005**, *127*, 17616–17617; j) C. Bakkali-Hassani, E. Rieger, J. Vignolle, F. R. Wurm, S. Carlotti, D. Taton, *Chem. Commun.* **2016**, *52*, 9719–9722; k) M. I. Childers, J. M. Longo, N. J. Van Zee, A. M. LaPointe, G. W. Coates, *Chem. Rev.* **2014**, *114*, 8129–8152; l) R. C. Ferrier Jr, S. Pakhira, S. E. Palmon, C. G. Rodriguez, D. J. Goldfeld, O. O. Iyiola, N. A. Lynd, *Macromolecules* **2018**, *51*, 1777–1786.

[3] a) L. Wu, Z. Armstrong, S. P. Schröder, C. de Boer, M. Artola, J. M. F. G. Aerts, H. S. Overkleeft, G. J. Davies, *Curr. Opin. Chem. Biol.* **2019**, *53*, 25–36; b) R. J. Rowland, Y. Chen, I. Breen, L. Wu, W. A. Offen, T. J. Beenakker, Q. Su, A. M. C. H. Nieuwendijk, J. M. F. G. Aerts, M. Artola, H. S. Overkleeft, G. J. Davies, *Chem. Eur. J.* **2021**, *27*, 16377–16388; c) N. G. S. McGregor, C. Kuo, T. J. M. Beenakker C Wong, W. A. Offen, Z. Armstrong, B. I. Florea, J. D. C. Codée, H. S. Overkleeft, J. M. F. G. Aerts, G. J. Davies, *Org. Biomol. Chem.* **2022**, *20*, 877–886; d) F. Christopher, Q. Shi, J. F. Fisher, M. Lee, D. Hesek, L. I. Llarrull, M. Toth, M. Gossing, R. Fridman, S. Mobashery, *Chem. Biol. Drug Des.* **2009**, *74*, 527–534; e) A. Tamburrini, C. Colombo, A. Bernardi, *Med. Res. Rev.* **2020**, *40*, 495–531; f) S. P. Schröder, W. W. Kallemeijn, M. F. Debets, T. Hansen, S. Hakki, S. J. Williams, T. J. Beenakker, J. M. Aerts, G. A. van der Marel, J. C. D. Codée, G. J. Davies, H. S. Overkleeft, *Chem. Eur. J.* **2018**, *24*, 9983–9992; g) X. BoTao, G. de Bruin, M. Verdoes, D. V. Filippov, G. A. van der Marel, H. S. Overkleeft, *Org. Biomol. Chem.* **2014**, *12*, 5710–5718; h) B. Daniel, Z. Kaczmarska, C. Arkona, R. Schulz, C. Tauber, G. Wolber, R. Hilgenfeld, M. Coll, J. Rademann, *Nat. Commun.* **2016**, *7*, 1–9; i) K. B. Sexton, D. Kato, A. B. Berger, M. Fonovic, S. H. Verhelst, M. Bogyo, *Cell Death Differ.* **2007**, *14*, 727–732.

[4] T. Hansen, P. Vermeeren, R. Yoshisada, D. V. Filippov, G. A. van der Marel, J. D. C. Codée, T. A. Hamlin, *J. Org. Chem.* **2021**, *86*, 3565–3573.

[5] a) H. D. Banks, *J. Org. Chem.* **2003**, *68*, 2639–2644; b) H. Helten, T. Schirmeister, B. Engels *J. Org. Chem.* **2005**, *70*, 233–237.

[6] a) T. Gleede, L. Reisman, E. Rieger, P. C. Mbarushimana, P. A. Rupar, F. R. Wurm, *Polym. Chem.* **2019**, *10*, 3257–3283; b) J. B. Sweeney, *Chem. Soc. Rev.* **2002**, *31*, 247–258; c) P. A. Evans, *Science of Synthesis, Volume 3: Stereoselective Synthesis 3*, Thieme, **2011**.

[7] L. F. Sobala, G. Speciale, S. Zhu, L. Raich, N. Sannikova, A. J. Thompson Zalihe, H. Z. Hakki, D. Lu, S. S. K. Abadi, A. R. Lewis, V. Rojas-Cervellera, G. Bernardo-Seisdedos, Y. Zhang, O. Millet, J. Jiménez-Barbero, A. J. Bennet, M. Sollogoub, C. Rovira, G. J. Davies, S. J. Williams *ACS Cent. Sci.* **2020**, *6*, 760–770.

[8] a) M. Sander, *Chem. Rev.* **1966**, *66*, 297–339; b) S. M. Bachrach, *J. Phys. Chem.* **1989**, *93*, 7780–7784; c) M. G. Beaver, S. B. Billings, K. A. Woerpel, *Eur. J. Org. Chem.* **2008**, *5*, 771–781; d) A. J. Plajer, C. K. Williams, *Angew. Chem. Int. Ed.* **2022**, *61*, e202104495; e) J. W. Li, M. Chen, Z. Zhang, C. Y. Pan, W. J. Zhang, C. Y. Hong, *Polym. Chem.* **2022**, *13*, 402–410; f) A. Espinosa Ferao, A. Rey Planells, R. Streubel, *Eur. J. Inorg. Chem.* **2021**, *2021*, 348–353; g) A. G. Alcaraz, A. E. Ferao, R. Streubel, *Dalton Trans.* **2021**, *50*, 7324–7336.

[9] a) P. E. Maligres, M. M. See, D. Askin, P. J. Reider, *Tetrahedron Lett.* **1997**, *38*, 5253–5256; b) P. C. Mbarushimana, Q. Liang, J. M. Allred, P. A. Rupar, *Macromolecules* **2018**, *51*, 977–983; c) M. K. Ghorai, A. Kumar, D. P. Tiwari, *J. Org. Chem.* **2010**, *75*, 137–151; d) M. K. Ghorai, A. K. Sahoo, S. Kumar, *Org. Lett.* **2011**, *13*, 5972–5975; e) M. K. Ghorai, D. P. Tiwari, N. Jain, *J. Org. Chem.* **2013**, *78*, 7121–7130.

[10] CP2K version 7.1, the CP2K developers group, **2019**, CP2K is freely available from https://www.cp2k.org.

[11] J. van de Vondele, M. Krack, F. Mohamed, M. Parrinello, T. Chassaing, J. Hutter, *Comput. Phys. Commun.* **2005**, *167*, 103–128.

[12] J. P. Perdew, K. Burke, M. Ernzerhof, *Phys. Rev. Lett.* **1996**, *77*, 3865–3868.

[13] M. Marianski, A. Supady, T. Ingram, M. Schneider, C. Baldauf, *J. Chem. Theory Comput.* **2016**, *12*, 6157–6168.

[14] J. van de Vondele, J. Hutter, *J. Chem. Phys.* **2007**, *127*, 114105.

[15] a) G. A. Tribello, M. Bonomi, D. Branduardi, C. Camilloni, G. Bussi, *Comp. Phys. Commun.* **2014**, *185*, 604–613; b) The PLUMED consortium. *Nat Methods* **2019**, *16*, 670–673.

[16] D. Cremer, J. A. Pople, *J. Am. Chem. Soc.* **1975**, *97*, 1354–1358.

[17] a) A. Ardèvol, C. Rovira, *J. Am. Chem. Soc.* **2015**, *137*, 7528–7547; b) J. Iglesias-Fernández, L. Raich, A. Ardèvol, C. Rovira, *Chem. Sci.* **2015**, *6*, 1167–1177.

[18] a) G. te Velde, F. M. Bickelhaupt, E. J. Baerends, C. Fonseca Guerra, S. J. A. van Gisbergen, J. G. Snijders, T. Ziegler, *J. Comput. Chem.* **2001**, *22*, 931–967; b) C. Fonseca Guerra, J. G. Snijders, G. te Velde, E. J. Baerends, *Theor. Chem. Acc.* **1998**, *99*, 391–403; c) ADF2019.302, SCM Theoretical Chemistry; Vrije Universiteit, Amsterdam (The Netherlands), http://www.scm.com.

[19] a) N. C. Handy, A. J. Cohen, *Mol. Phys.* **2001**, *99*, 403; b) C. Lee, W. Yang, R. G. Parr, *Phys. Rev. B: Condens. Matter Mater. Phys.* **1988**, *37*, 785.

[20] a) A. P. Bento, F. M. Bickelhaupt, M. Solà, *J. Chem. Theory Comput.* **2008**, *4*, 929–940; b) M. Swart, M. Solà, F. M. Bickelhaupt, *J. Chem. Theory Comput.* **2010**, *6*, 3145–3152.

[21] E. van Lenthe, E. J. Baerends, J. G. Snijders, *J. Chem. Phys.* **1994**, *101*, 9783.–9792.

[22] E. van Lenthe, E. J. Baerends, *J. Comput. Chem.* **2003**, *24*, 1142–1156.

[23] a) M. Franchini, P. H. T. Philipsen, E. van Lenthe, L. Visscher, *J. Chem. Theory Comput.* **2014**, *10*, 1994–2004; b) M. Franchini, P. H. T. Philipsen, L. Visscher, *J. Comput. Chem.* **2013**, *34*, 1819–1827.

[24] a) A. Bérces, R. M. Dickson, L. Fan, H. Jacobsen, D. Swerhone, T. Ziegler, *Comput. Phys. Commun.* **1997**, *100*, 247–262; b) H. Jacobsen, A. Bérces, D. P. Swerhone, T. Ziegler, *Comput. Phys. Commun.* **1997**, *100*, 263–276; c) S. K. Wolff, *Int. J. Quantum Chem.* **2005**, *104*, 645–659.

[25] a) L. Deng, T. Ziegler, *Int. J. Quantum Chem.* **1994**, *52*, 731–765; b) L. Deng, T. Ziegler, L. Fan, *J. Chem. Phys.* **1993**, *99*, 3823–3835; c) K. Fukui, *Acc. Chem. Res.* **1981**, *14*, 363–368.

[26] a) X. Sun, T. M. Soini, J. Poater, T. A. Hamlin, F. M. Bickelhaupt, *J. Comput. Chem.* **2019**, *40*, 2227–2233; b) X. Sun, T. Soini, L. P. Wolters, W.-J. van Zeist, C. Fonseca Guerra, T. A. Hamlin, F. M. Bickelhaupt, PyFrag 2007–2022, Vrije Universiteit Amsterdam (The Netherlands).

Chemistry–A European Journal

Research Article
doi.org/10.1002/chem.202201649

Chemistry Europe
European Chemical
Societies Publishing

[27] C. Y. Legaut, CYLview, 1.0b; Université de Sherbrooke, QC (Canada), **2009**, http://www.cylview.org.

[28] a) P. Vermeeren, S. C. C. van der Lubbe, C. Fonseca Guerra, F. M. Bickelhaupt, T. A. Hamlin, *Nat. Protoc.* **2020**, *15*, 649–667; b) P. Vermeeren, T. A. Hamlin, F. M. Bickelhaupt, *Chem. Commun.* **2021**, *57*, 5880–5896.

[29] a) D. H. Ess, K. N. Houk, *J. Am. Chem. Soc.* **2007**, *129*, 10646–10647; b) D. H. Ess, K. N. Houk, *J. Am. Chem. Soc.* **2008**, *130*, 10187–10198.

[30] a) F. M. Bickelhaupt, E. J. Baerends in *Reviews in Computational Chemistry, Vol. 15* (Eds.: K. B. Lipkowitz, D. B. Boyd), Wiley-VCH, New York, **2000**, pp 1–86; b) R. van Meer, O. V. Gritsenko, E. J. Baerends, *J. Chem. Theory Comput.* **2014**, *10*, 4432–4441.

[31] a) T. Hansen, P. Vermeeren, A. Haim, M. J. H. van Dorp, J. D. C. Codée, F. M. Bickelhaupt, T. A. Hamlin, *Eur. J. Org. Chem.* **2020**, *25*, 3822–3828; b) P. Vermeeren, T. Hansen, P. Jansen, M. Swart, T. A. Hamlin, F. M. Bickelhaupt, *Chem. Eur. J.* **2020**, *26*, 15538–1554; c) T. Hansen, J. C. Rooze, F. M. Bickelhaupt, T. A. Hamlin, *J. Org. Chem.* **2022**, *87*, 1805–1813; d) T. Hansen, P. Vermeeren, F. M. Bickelhaupt, T. A. Hamlin, *Angew. Chem.* **2021**, *133*, 21008–21016; *Angew. Chem. Int. Ed.* **2021**, *60*, 20840–20848; e) P. Vermeeren, T. Hansen, M. Grasser, D. R. Silva, T. A. Hamlin, F. M. Bickelhaupt, *J. Org. Chem.* **2020**, *85*, 14087–14093; f) T. Hansen, P. Vermeeren, L. de Jong, F. M. Bickelhaupt, T. A. Hamlin, *J. Org. Chem.* **2022**, *87*, 8892–8901.

[32] R. M. Ibberson, O. Yamamuro, I. Tsukushi, *Chem. Phys. Lett.* **2006**, *423*, 454–458.

[33] a) G. J. Davies, A. Planas, C. Rovira, *Acc. Chem. Res.* **2012**, *45*, 308–316; b) M. Artola, L. Wu, M. J. Ferraz, C. L. Kuo, L. Raich, I. Z. Breen, W. A. Offen, J. D. C. Codée, G. A. van der Marel, C. Rovira, J. M. Aerts, *ACS Cent. Sci.* **2017**, *3*, 784–793; c) T. J. Beenakker, D. P. Wander, W. A. Offen, M. Artola, L. Raich, M. J. Ferraz, K. Y. Li, J. H. Houben, E. R. van Rijssel, T. Hansen, G. A. van der Marel, J. D. C. Codée, J. M. F. G. Aerts, C. Rovira, G. J. Davies, H. S. Overkleeft, *J. Am. Chem. Soc.* **2017**, *139*, 6534–6537.

[34] a) D. M. Pawar, E. A. Noe, *J. Am. Chem. Soc.* **1998**, *120*, 1485–1488; b) F. R. Jensen, C. H. Bushweller, *J. Am. Chem. Soc.* **1969**, *91*, 5774–5782.

[35] a) T. A. Hamlin, T. A. M. Swart, F. M. Bickelhaupt, *ChemPhysChem* **2018** *19*, 1315–1330; b) F. M. Bickelhaupt, *Mass Spectrom. Rev.* **2001**, *20*, 347–361.

[36] C. Hansch, A. Leo, R. W. Taft, *Chem. Rev.* **1992**, *91*, 165–195.

[37] a) A. Klamt, G. Schüürmann, *J. Chem. Soc. Perkin Trans. 2* **1993**, 799; b) A. Klamt, *J. Phys. Chem.* **1995**, 2224; c) A. Klamt, V. Jonas, *J. Chem. Phys.* **1996**, *105*, 9972; d) C. C. Pye, T. Ziegler, *Theor. Chem. Acc.* **1999**, *101*, 396.

[38] a) P. Georgieva, F. Imo, *J. Comb. Chem.* **2010**, *31*, 1707–1714; b) P. Kukic, D. Farrell, L. P. McIntosh, E. B. García-Moreno, K. S. Jensen, Z. Toleikis, K. Teilum, J. E. Nielsen, *J. Ac. Chem. Soc.* **2013**, *135*, 16968–16976; c) E. L. Mertz, L. I. Krishtalik, *PNAS* **2000**, *97*, 2081–2086; d) N. C. Schutz, A. Warshel, *Proteins Struct. Funct. Genet.* **2001**, *44*, 400–417.

[39] Note, we do want to emphasize that the nature and type of the exact enzyme pocket will significantly influence the actual polarity of the enzyme environment.

[40] a) D. Svatunek, T. Hansen, K. N. Houk, T. A. Hamlin, *J. Org. Chem.* **2021**, *86*, 4320–4325; b) A. van der Ham, T. Hansen, G. Lodder, J. D. C. Codée, T. A. Hamlin, D. V. Filippov, *ChemPhysChem* **2019**, *20*, 2103–2109; c) T. Hansen, X. Sun, M. Dalla Tiezza, W. J. van Zeist, J. Poater, T. A. Hamlin, F. M. Bickelhaupt, *Chem. Eur. J.* **2022**, *28*, e202103953.

[41] Y. R. Luo, J. A. Kerr, Bond dissociation energies. *CRC handbook of chemistry and physics*, **2012**.

[42] E. Blokker, X. Sun, J. Poater, J. M. van der Schuur, T. A. Hamlin, F. M. Bickelhaupt, *Chem. J. Eur.* **2021**, *27*, 15616–15622.

[43] W.-J. van Zeist, F. M. Bickelhaupt, *Phys. Chem. Chem. Phys.* **2009**, *11*, 10317–10322.

[44] a) T. A. Hamlin, F. M. Bickelhaupt, I. Fernández, *Acc. Chem. Res.* **2021**, *54*, 1972–1981; b) P. Vermeeren, T. A. Hamlin, I. Fernández, F. M. Bickelhaupt, *Angew. Chem.* **2020**, *132*, 6260–6265; *Angew. Chem. Int. Ed.* **2020**, *59*, 6201–6206; c) P. Vermeeren, T. A. Hamlin, I. Fernández, F. M. Bickelhaupt, *Chem. Sci.* **2020**, *11*, 8105–811; d) E. H. Tiekink, P. Vermeeren, F. M. Bickelhaupt, T. A. Hamlin, *Eur. J. Org. Chem.* **2021**, *37*, 5275–5283.